Metabolic origins of spatial organization in the tumor microenvironment

Carlos Carmona-Fontaine[a,b,1], Maxime Deforet[a], Leila Akkari[c,d,e], Craig B. Thompson[c,1], Johanna A. Joyce[c,d,e], and Joao B. Xavier[a,1]

[a]Computational and Systems Biology Program, Memorial Sloan Kettering Cancer Center, New York, NY 10065; [b]Center for Genomics and Systems Biology, Department of Biology, New York University, New York, NY 10003; [c]Cancer Biology & Genetics Program, Memorial Sloan Kettering Cancer Center, New York, NY 10065; [d]Department of Oncology, University of Lausanne, 1066 Lausanne, Switzerland; and [e]Ludwig Institute for Cancer Research, University of Lausanne, 1066 Lausanne, Switzerland

Contributed by Craig B. Thompson, January 17, 2017 (sent for review December 13, 2016; reviewed by Jason W. Locasale and Ruslan Medzhitov)

The genetic and phenotypic diversity of cells within tumors is a major obstacle for cancer treatment. Because of the stochastic nature of genetic alterations, this intratumoral heterogeneity is often viewed as chaotic. Here we show that the altered metabolism of cancer cells creates predictable gradients of extracellular metabolites that orchestrate the phenotypic diversity of cells in the tumor microenvironment. Combining experiments and mathematical modeling, we show that metabolites consumed and secreted within the tumor microenvironment induce tumor-associated macrophages (TAMs) to differentiate into distinct subpopulations according to local levels of ischemia and their position relative to the vasculature. TAMs integrate levels of hypoxia and lactate into progressive activation of MAPK signaling that induce predictable spatial patterns of gene expression, such as stripes of macrophages expressing arginase 1 (ARG1) and mannose receptor, C type 1 (MRC1). These phenotypic changes are functionally relevant as ischemic macrophages triggered tube-like morphogenesis in neighboring endothelial cells that could restore blood perfusion in nutrient-deprived regions where angiogenic resources are most needed. We propose that gradients of extracellular metabolites act as tumor morphogens that impose order within the microenvironment, much like signaling molecules convey positional information to organize embryonic tissues. Unearthing embryology-like processes in tumors may allow us to control organ-like tumor features such as tissue repair and revascularization and treat intratumoral heterogeneity.

cancer metabolism | tumor microenvironment | morphogens | positional information | tumor-associated macrophages

Tumors display a large degree of genetic and phenotypic heterogeneity that hampers diagnosis and treatment (1–8). However, tumors are capable of local organization and respond collectively to signals from their microenvironment (9, 10). Examples include the formation of multicellular structures such as blood vessels (11, 12), coordinated collective invasion (13), noncell autonomous paracrine effects (14), and "division of labor" between different tumor cells (15). How can multicellular organization emerge within heterogeneous and genetically diverse tumors?

Here we reveal that gradients of metabolites, formed by the altered metabolism of cancer cells (16–18) and accentuated by aberrant vascularization (11, 19–21), lead to predictable phenotypic diversity in the tumor microenvironment. This drives temporal and spatial coordination of multiple cell types, including tumor-associated macrophages (TAMs) that are known to respond to extracellular metabolite levels (21–24). We propose that the topology of the vasculature leads to local differences in metabolite concentrations that provide spatial information that can modulate the phenotypes of different cells in the tumor microenvironment.

Results

Extracellular Metabolites Form Gradients That Convey Positional Information in Tumors. To measure intratumoral cellular heterogeneity, while preserving information regarding tissue microarchitecture, we developed an image cytometry approach that combines multiscale microscopy and image processing to extract single-cell data, including spatial features such as distance to the vasculature, for thousands of cells in tumor tissue cryosections (Fig. 1*A* and Fig. S1 *A–D*). In a mouse model of breast tumor [mouse mammary tumor virus–polyoma virus middle T-antigen (MMTV-PyMT)] we found that gradients of hypoxia [labeled with pimonidazole (PMO)] closely mirrored the topology of the vasculature and, consistent with previous reports (12, 19–21), saturated at ∼100 μm from the closest blood vessel (Fig. 1 *B* and *C*).

We asked whether these gradients of metabolites could impose patterned phenotypic changes in cells experiencing different local conditions. We focused on TAMs, a major protumoral stromal infiltrate (25–27) whose phenotypic state and viability can be altered by metabolic stimuli (21–23). We measured levels of selected markers associated with different TAM states and investigated their relationship to local hypoxia levels and distance to the nearest vessel. Whereas some macrophage markers were expressed homogenously (Fig. S1*E*), the TAM markers arginase 1 (ARG1) and mannose receptor, C type 1 (MRC1) were expressed in distinct and spatially restricted subpopulations (Fig. 1*D*). TAMs located in well-nourished regions, such as cortical and perivascular areas, expressed MRC1 whereas

Significance

Cancers appear as disordered mixtures of different cells, which is partly why they are hard to treat. We show here that despite this chaos, tumors show local organization that emerges from cellular processes common to most cancers: the altered metabolism of cancer cells and the interactions with stromal cells in the tumor microenvironment. With a multidisciplinary approach combining experiments and computer simulations we revealed that the metabolic activity of cancer cells produces gradients of nutrients and metabolic waste products that act as signals that cells use to know their position with respect to blood vessels. This positional information orchestrates a modular organization of tumor and stromal cells that resembles embryonic organization, which we could exploit as a therapeutic target.

Author contributions: C.C.-F., C.B.T., J.A.J., and J.B.X. designed research; C.C.-F., M.D., and L.A. performed research; C.C.-F. analyzed data; and C.C.-F. and C.B.T. wrote the paper.

Reviewers: J.W.L., Duke University; and R.M., Yale University School of Medicine.

Conflict of interest statement: C.B.T. is a founder of Agios Pharmaceuticals and a member of its scientific advisory board. He also serves on the board of directors of Merck and Charles River Laboratories.

Freely available online through the PNAS open access option.

Data deposition: The sequences reported in this paper have been deposited in the Gene Expression Omnibus (GEO) database, www.ncbi.nlm.nih.gov/geo (accession no. GSE93702).

[1]To whom correspondence may be addressed. Email: carlos.carmona-fontaine@nyu.edu, thompsonc@mskcc.org, or xavierj@mskcc.org.

This article contains supporting information online at www.pnas.org/lookup/suppl/doi:10.1073/pnas.1700600114/-/DCSupplemental.

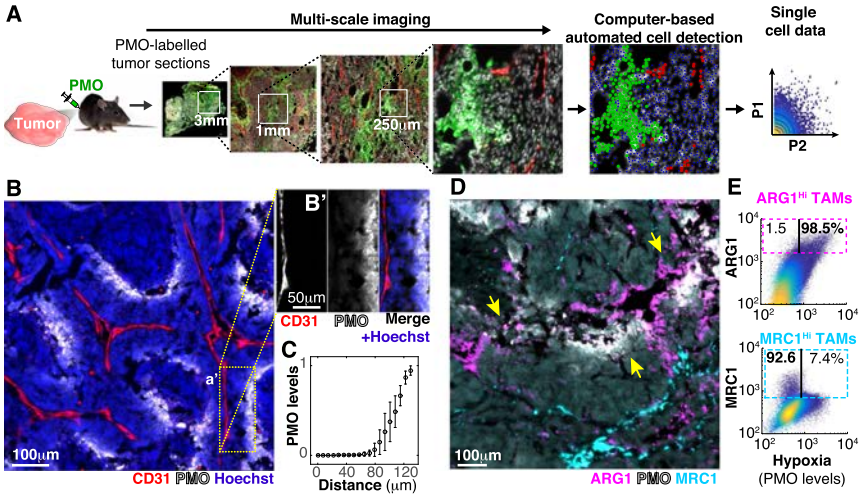

Fig. 1. Spatial diversity in TAM phenotypes correlates with metabolic gradients within tumors. (*A*) Experimental approach to study metabolic and cellular intratumoral heterogeneity. PMO (a hypoxia marker) was injected into tumor-bearing mice to label hypoxic tumor regions. Tumor cryosections were then imaged at high magnification (typically at 200×), achieving multiscale images. This enabled image processing to obtain single-cell features for hundreds of thousands of cells per section while maintaining their spatial information. (*B* and *C*) The spatial distribution of hypoxia mirrored the structure of the tumor vasculature from a distance. (*B*) Cryosections of MMTV-PyMT tumors were stained with antibodies against endothelial vascular cells (CD31) and hypoxic regions (PMO). (*B′*) Image channels were split in a selected field of interest to reveal the correlation between hypoxia and distance from the vessel. This was quantified in *C* (bars indicate SD, $n = 6$). (*D* and *E*) Phenotypic diversity of TAMs correlates with the topology of the vascular system. (*D*) Similar tissue sections were stained with antibodies against TAM markers (MRC1 and ARG1) and PMO (colocalization of ARG1 and PMO indicated by yellow arrows). (*E*) Image quantification of $>10^5$ individual cells within tumor sections showed that ARG1 levels in TAMs were correlated with hypoxic regions ($r = 0.6$, $P < 10^{-6}$) whereas MRC1-expressing TAMs were inversely correlated with local hypoxic levels ($r = -0.2$, $P < 10^{-6}$). Three sections of three tumors extracted from different animals were analyzed for each marker.

macrophages within hypoxic regions, far from the vasculature, showed high ARG1 protein levels (Fig. 1 *D* and *E*). The spatial segregation between $ARG1^{HI}$ and $MRC1^{HI}$ TAMs was somewhat surprising because these markers are often coexpressed by antiinflammatory macrophages that respond to type 2 helper T-cell (T_h2) signals and have been proposed to share features with TAMs (26–29). We confirmed the correlation between hypoxia and the location of $ARG1^{HI}$ TAMs in a mouse model of pancreatic neuroendocrine tumors [rat insulin promoter 1–T-antigen (RIP1-TAg2)] (Fig. S1*F*), indicating that spatial patterning of TAM phenotypes is a common feature of the tumor microenvironment.

Gradients of Oxygen and Lactate Orchestrate Spatial Patterns of Cell Phenotypes. Our in vivo observations suggest a model where extracellular metabolites specify different TAM subpopulations across concentration gradients, similar to how morphogen gradients specify stripes of gene expression during embryonic development (30–32). We then sought to investigate whether metabolite gradients were sufficient to produce gene expression patterns in TAMs. Traditional in vitro systems are spatially homogeneous without major changes in metabolite distribution. To overcome this, we developed an in vitro microphysiological system named the metabolic microenvironment chamber (MEMIC) (Fig. 2*A* and Fig. S2 *A* and *B*). MEMIC allows gradients of ischemia to emerge spontaneously as a result of cellular activities such as nutrient consumption and secretion of waste products. As a proof of principle, we used MEMIC to generate and visualize oxygen gradients in the hypoxic response of C6 glioma cells engineered to express GFP under an HIF1α-responsive element (C6-GFP-HRE) (21) (Fig. 2*B*).

To assess whether gradients of metabolites can pattern macrophages in the MEMIC, we cultured bone marrow-derived macrophages (hereafter referred to simply as macrophages) (*SI Materials and Methods*) with C6-GFP-HRE cells. After 24 h, macrophages showed spatial patterns of ARG1 protein levels that correlated with GFP (hypoxia) and increased with the distance to the normoxic region (Fig. 2 *C* and *D*). In control experiments lacking metabolite gradients, we did not observe induction of ARG1 expression (Fig. 2*D*). Consistent with our in vivo observations, MRC1 protein levels were inversely correlated with hypoxia and were higher in normoxic regions (Fig. 2*E* and Fig. S2*C*). These spontaneous expression patterns were not dependent on the cancer cell type as MEMIC experiments with macrophages cocultured with cell lines derived from the PyMT and Rip-Tag2 tumor models used above, human cancer cell lines (Fig. S2 *C* and *D*), or even macrophages cultured alone (Fig. 2*F*) showed the same trend. We have recently shown that extreme levels of ischemia are lethal for macrophages (21). Consistently, ARG1 expression emerges as a stripe between well-nurtured macrophages and the region where ischemic levels become lethal (Fig. 2*F*). Together, these results demonstrate that MEMIC experiments suggest that extracellular metabolite gradients play a key role in the phenotypic diversity of TAMs.

Gradual changes in metabolite concentration are somehow translated into discrete stripes of gene expression patterns with clear boundaries (Fig. 2*F* and Fig. S2*C*). To identify which metabolites are setting these phenotypic boundaries, we focused on the ischemic $ARG1^{HI}/MRC1^{LO}$ macrophage subpopulation. First, we wanted to separate the effect of hypoxia from other ischemic conditions such as nutrient deprivation. To do this, we cultured macrophages within a modified MEMIC where the top cover was made permeable to oxygen but not to soluble metabolites. In this scenario, ARG1 protein levels remained low across the entire MEMIC, showing that hypoxia is necessary to produce ARG1 patterns (Fig. 2*G*). To test whether hypoxia was sufficient to induce ARG1, we cultured macrophages in regular culture plates within a hypoxic chamber (1% oxygen) or under normal cell culture conditions (21% oxygen). Surprisingly, we found no effect of hypoxia in ARG1 levels, unless macrophages were cultured at high cell densities (Fig. 2*H*), indicating that hypoxia was necessary but not sufficient to pattern macrophages. This cell density effect was not mediated by cell–cell contact because stimulation of cell contact-sensing molecules (33) did not increase ARG1 levels (Fig. S3*A*).

Consistent with previous evidence (22), we found extensive evidence for the synergistic role of hypoxia and lactate. First, the treatment of sparse macrophage populations with a combination of hypoxia and culture media previously conditioned by dense macrophage populations (cultured under hypoxia) increased ARG1 levels (Fig. 2*I*). To determine the molecular weight of the secreted signal, we fractionated the conditioned media (3-kDa cutoff columns). This revealed that the low, but not the high, molecular weight fraction of the conditioned media increased ARG1 levels in sparse macrophage cultures, indicating that the sensed factor was a small molecule (Fig. 2*I*). We therefore screened for different small molecules that could synergize with hypoxia to increase ARG1 levels (Table S1). We found

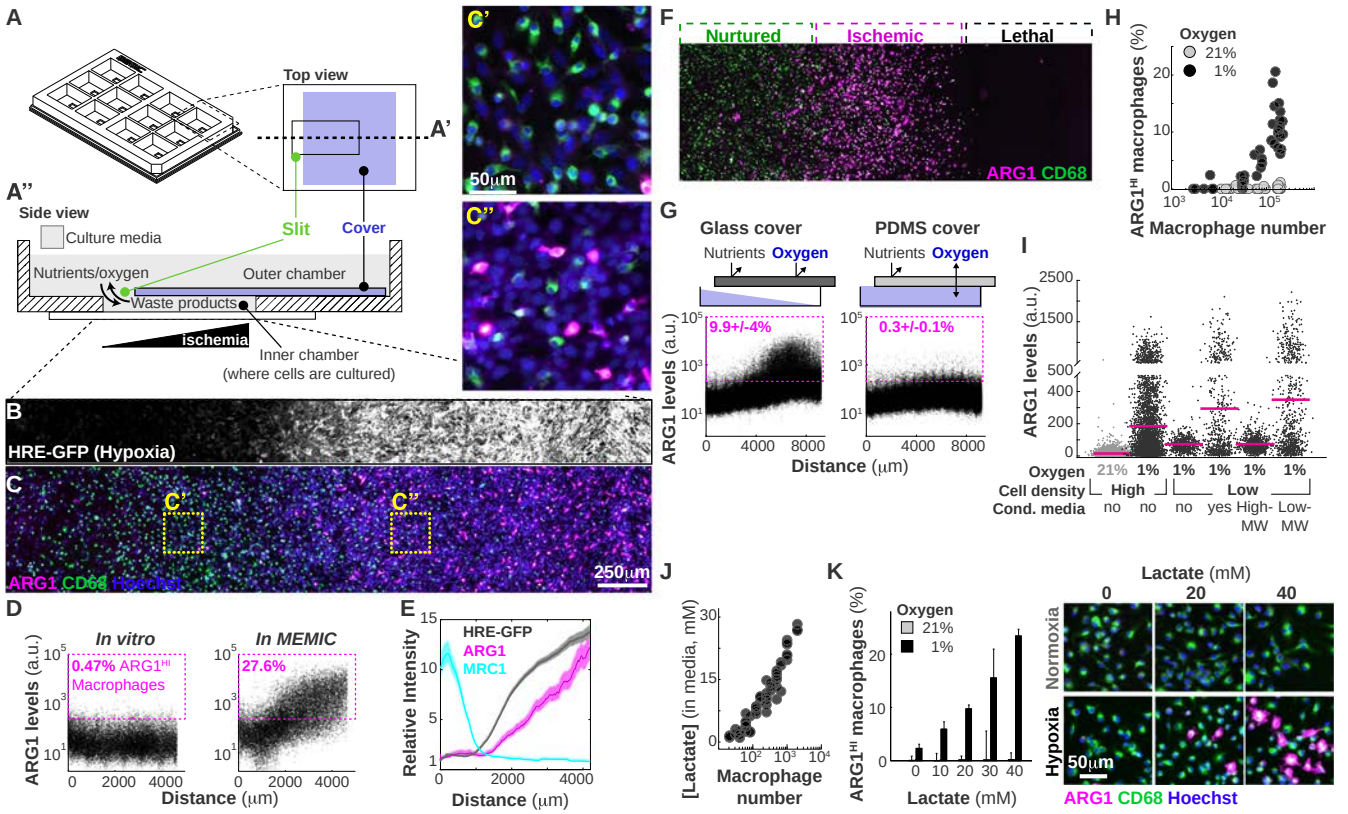

Fig. 2. Extracellular metabolic gradients are necessary and sufficient to produce striped expression domains and spatial patterning of macrophages. (*A*) Schematic representation of the MEMIC chamber fabricated with 3D printing. This 12-well format contains an independent MEMIC replicate in each well. (*A′*) Top view of one of those wells. (*A″*) Detailed side view of a MEMIC where cells are cultured in a small chamber that connects to a large volume of fresh media through a slit. Cell activities such as nutrient consumption and waste product secretion change the local nutrient composition within the small chamber and generate spatial gradients; diffusion via the slit allows a constant exchange with the fresh media reservoir. Thus, cells proximal to this slit remain well nurtured, whereas distal cells become progressively more ischemic. (*B* and *C*) Coculture of macrophages and a cancer cell line engineered to express GFP under hypoxia (C6-HRE-GFP). (*B*) GFP hypoxia at 24 h reveals a spatial gradient. (*C*) In the same culture, spatial patterns of ARG1 in macrophages mirrored hypoxia gradients (compare *Insets C′* and *C″*). (*D*) Image analysis at the single-cell level of macrophages cocultured with C6-HRE-GFP glioma cells in a conventional in vitro system (without metabolite gradients, *Left*) or in the MEMIC (*Right*). ARG1^{HI} macrophages are defined as expressing levels fivefold higher than the median. (*E*) ARG1 levels increased with hypoxia whereas MRC1 levels decreased with hypoxia. (*F–H*) Hypoxia was necessary but not sufficient to trigger ARG1 expression. (*F*) Cancer cells were not required for the emergence of phenotypic patterns as macrophages cultured in the MEMIC alone displayed stripes of ARG1 expression in sublethal levels of ischemia. (*G*) Spatial patterns of ARG1 expression in macrophage monocultures (*Left*). This effect required hypoxia as it disappeared when O_2 concentration was restored to environmental levels using a polydimethylsiloxane (PDMS) membrane (*Right*) that is permeable to gases. (*H*) Hypoxia can induce the expression of ARG1 but only in high-density cultures, showing that it is necessary but not sufficient. (*I*) Low molecular weight fraction of conditioned media collected from macrophages cultured under hypoxia can trigger ARG1 expression in sparse macrophage cultures. Conditioned media were fractioned according to molecular weight (MW) with a 3-kDa cutoff. Note change of scale in *y* axis. (*J*) Lactate, which accumulated in the cell culture media of hypoxic macrophages, increases with macrophage density (24 h culture at 1% O_2). (*K*) Lactate showed a dose-dependent synergy in inducing ARG1 levels with low O_2. Lactate doses were chosen to cover the range between no lactate and high lactate doses typically used to study cellular response to this molecule (21, 22, 48). Bars indicate SD from three biological replicates. Images are representative of selected lactate doses.

that the most potent inducer was lactate (Fig. S3*B*). Hypoxic macrophages secreted lactate, which accumulated in the cell culture media proportionally to the density of macrophages (Fig. 2*J*). When we treated normoxic and hypoxic macrophages with a wide range of lactate doses, we saw a concomitant increase of ARG1 protein levels in hypoxic macrophages but not in normoxic ones, showing that lactate and hypoxia act as synergistic cues to induce ARG1 expression (Fig. 2*K*). This effect is consistent with recent evidence showing a similar effect of lactate in transcription levels of *Arg1* mRNA in TAMs (22). However, in our experiments, lactate alone was not sufficient to trigger a maximal *Arg1* response at the protein level (Fig. 2*K*).

Lactic acid had similar effects to those of lactate but at high concentrations it also affected macrophage viability due to media acidification (21) (Fig. S3 *C–E*). Overall, our results showed that a combination of low oxygen and high lactate was necessary and sufficient to trigger the expression of ARG1 in macrophages. These data suggest that opposing gradients of lactate and oxygen, which are ubiquitous in solid tumors (19–21), create predictable phenotypic patterns among TAMs. Because these gradients follow the topology of the tumor vascular system (Fig. 1), it is possible that they convey positional information about the distance to blood vessels.

Positional Information Is Interpreted via MAPK/ERK Signaling. We then investigated how macrophages sensed the combination of low oxygen and high lactate and integrated those signals into phenotypic responses. We used RNA sequencing (RNA-seq) to identify transcriptional differences between macrophages treated with different levels of oxygen and/or high lactate (Fig. 3*A* and Fig. S3 *A–C*). We first observed that transcriptional changes in macrophages treated by oxygen/lactate did not display a consistent change in gene expression of markers commonly used to characterize macrophages as pro- or antiinflammatory (26–29) in a consistent manner (Fig. S4*C*). The effect of metabolites, however, did induce features of the Toll-like receptor 4 (TLR4)-induced

macrophage response to LPS that signals via the MAPK pathway (Fig. S4 *C* and *D*), such as *Arg1* and *Nos2* coexpression (34). Reinforcing this observation, gene set enrichment analysis (GSEA) of RNA-seq data revealed that macrophages cultured in low oxygen and high lactate showed an enriched signature of KRAS/MAPK signaling activation (Fig. 3*A* and Fig. S4*F*). Pharmacological perturbations further supported a role for the MAPK pathway by showing that LPS increased ARG1 levels in hypoxic macrophages specifically through this pathway (Fig. S4 *E*–*H*).

If the MAPK pathway is interpreting positional information brought by oxygen and lactate gradients, it should (*i*) be activated in a gradual manner and (*ii*) be required for the phenotypic switch we observed in macrophages (35, 36). First, we observed a strong correlation between phospho-ERK1/2 levels and the distance from the normoxic region (Fig. 3*B*) whereas total MAPK (ERK1/2) levels remained constant (Fig. S4*I*). Inhibition of MEK, a key member of this pathway, completely abrogated ARG1 patterning (Fig. 3*C*). Similar results were obtained by inhibiting the upstream MAPK component c-Raf with the Food and Drug Administration (FDA)-approved inhibitor Sorafenib as well as with the more selective GW5074 (Fig. S4*K*). Altogether our data show that, by sensing lactate and oxygen levels, TAMs can determine their position with respect to the vasculature (or to the slit in the MEMIC). This positional information required MAPK signaling and led to a predictable emergence of spatial phenotypic diversity in macrophages.

Macrophages Relay Positional Information and Organize Morphogenetic Changes in Neighboring Cells. During embryogenesis, patterned cells can elaborate and refine developmental programs by relaying their positional information via the secretion of cell signals that are sensed by adjacent cells (30–32). We thus hypothesized that macrophages, conditioned by metabolic cues, can relay their positional information to neighboring cells (Fig. 4*A*). We thus compared cytokine secretion profiles of macrophages treated with hypoxia and/or high levels of lactate. The combination of hypoxia and lactate increased secretion of the proangiogenic cytokine VEGFA above all other 111 screened cytokines (Fig. 4*B*). Quantification of secreted VEGFA, using a bead-based ELISA (Fig. 4*C*), and of *Vegfa* mRNA levels, using quantitative PCR (qPCR) (Fig. S4*D*), showed that hypoxia increased VEGFA secretion and that this effect was boosted by lactate, indicating that hypoxia and lactate regulate macrophage cytokine production in a synergistic manner (Fig. S4*J*).

To test whether these changes were functionally relevant, we cocultured GFP-expressing macrophages with mCherry-labeled SVEC4-10 endothelial (SVEC) cells embedded in a matrigel/collagen I matrix layer (Fig. S5*B*). Under normal conditions, these cocultures did not result in any evidence of vasculogenesis. In contrast, macrophages previously cultured under low oxygen and high lactate levels were able to induce tube-like morphogenesis in SVEC cells (Fig. S5*B* and Movie S1). Control experiments using hypoxia and lactate in the absence of macrophages or in the presence of macrophages treated with MAPK or VEGF inhibitors showed no vascular morphogenesis, indicating that VEGFA, secreted by ischemic macrophages, was required for the response of endothelial cells (Fig. S5*C*). These data show that macrophages were able to relay information about microenvironmental conditions to endothelial cells and to trigger a modular and noncell autonomous process of tube-like morphogenesis in response to oxygen and lactate levels.

Positional Information Optimizes Angiogenesis and Leads to Faster-Growing Tumors. Lactate and hypoxia increase with the distance from the vasculature, suggesting that VEGFA levels should also increase within ischemic regions. Using an agent-based model that we developed to study this type of question (21), we predicted that VEGFA levels should indeed increase in ischemic regions (Fig. 4*D*). Consistent with this, analysis of tumor sections in the MMTV-PyMT model revealed that hypoxic TAMs expressed higher VEGFA levels than TAMs located in other tumor regions (Fig. 4*E*). We also observed that within hypoxic tumor regions, VEGFA-expressing TAMs were associated with small groups of $CD31^+$ endothelial cells that have not yet formed into vessels (Fig. 4*F*). These endothelial cells stained positive for the nascent capillary marker nestin (NES) (Fig. S5*A*). A similar scenario has been reported during nerve regeneration where hypoxia triggers VEGFA secretion by resident macrophages that then recruit endothelial cells required for revascularization and repair (23, 37). Our data suggest that ischemic TAM subpopulations secrete VEGFA to induce endothelial cells to initiate the revascularization of nutrient-deprived tumor regions, which in turn would promote tumor growth (Fig. 4*G*). In fact, the metabolism of TAMs has been recently shown to control tumor blood vessel morphogenesis and metastasis (24).

Is there any advantage for the tumor to maintain a spatially regulated vascularization mechanism? How does it compare, for example, to constitutive secretion of VEGFA that would promote angiogenesis throughout the tumor? With the help of mathematical modeling, we first simulated the growth of tumors with a responsive angiogenic strategy, where the secretion of proangiogenic factors (e.g., VEGFA) is modulated by extracellular metabolites, which we compared with simulated tumors that used a constitutive proangiogenic strategy. We assumed that (*i*) the benefits of vascularization (i.e., nutrients, oxygen) have diminishing returns on cell growth (i.e., excessive nutrients no longer increase cell growth rate) and (*ii*) the formation of new vessels is a costly process. We implemented this as an explicit cost, but it can also result from the increasing resistance to flow in a dense vascular network (38). The analytical solution to this model revealed that the responsive strategy always led to faster tumor growth rates even though the total levels of VEGFA were higher in the constitutive model (Fig. 4 *H* and *I* and Fig. S6*A*). More detailed agent-based models confirmed these conclusions (Fig. S6 *B*–*E*, Movie S2, and Fig. 4 *J* and *K*; model details in *Supporting Information, Mathematical Modeling*). This result highlights that the spatial

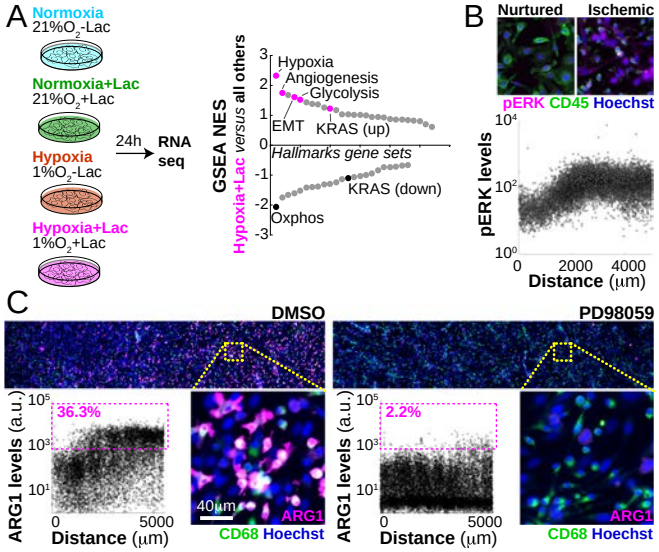

Fig. 3. Macrophages respond to gradients of extracellular metabolites, using MAPK signaling. (*A*) RNA-seq revealed transcriptional changes of macrophages cultured under different levels of metabolites. GSEA suggested a strong enrichment of the KRAS/MAPK pathway. (*B*) KRAS signals via the MAPK pathway and macrophages cultured in the MEMIC showed spatial patterns of MAPK activation (ERK1/2 phosphorylation) correlated with ischemia. (*C*) Representative images and single-cell–level quantification showing that MAPK inhibition abrogates macrophage spatial patterns in the MEMIC.

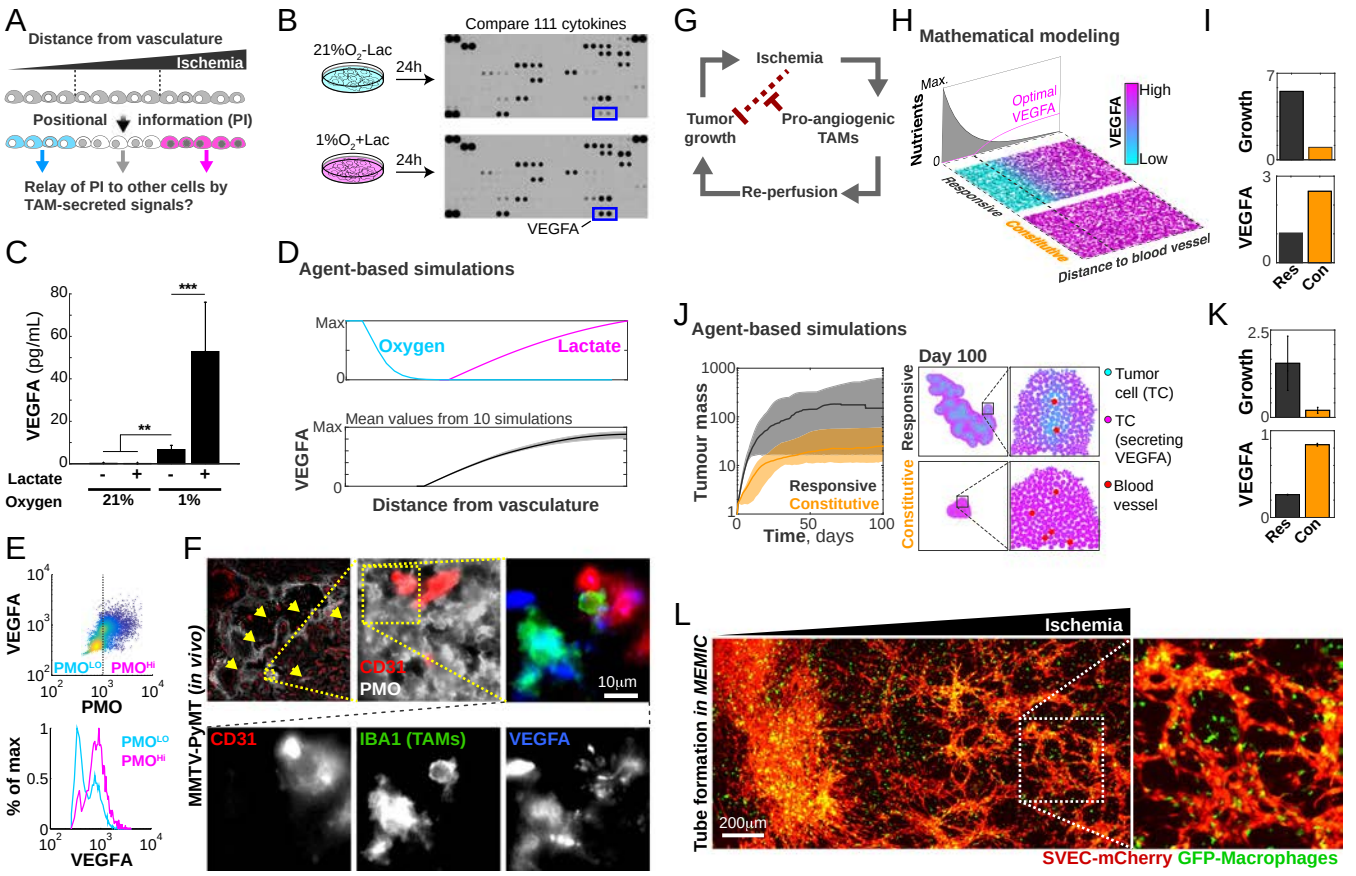

Fig. 4. Macrophages relay their positional information to endothelial cells and orchestrate efficient tube morphogenesis. (*A*) Our data suggest that, in a process resembling embryological organization, gradients of extracellular metabolites convey positional information that modifies TAM phenotypes. We asked whether additional signaling molecules, secreted by patterned macrophages, could relay positional information to other tumor cells. (*B*) Screening of 111 secreted chemokines revealed that ischemic macrophages express VEGFA. (*C*) Quantification of secreted chemokines confirmed this finding and the synergy between lactate and hypoxia (bars indicate SD from six biological replicates; $^{**}P < 0.01$, $^{***}P < 0.001$). (*D*) Mathematical modeling predicted spatial patterns of VEGFA levels. (*E*) Quantification in a representative PyMT-MMTV tumor section showing that ischemic TAMs express higher VEGFA levels. (*F*) Images showing small groups of endothelial cells in hypoxic regions (yellow arrows). One of these regions was magnified to show that these endothelial cells are adjacent to VEGFA-expressing TAMs. For clarity, *F*, *Lower* shows isolated channels. (*G*) Our data suggest that whereas tumor growth leads to ischemic regions, the response of the stroma is to revascularize these regions, thus allowing tumor growth to resume. (*H* and *I*) Analytical solution of our theoretical model showed that a proangiogenic strategy that responds to ischemia (Res, responsive) led to faster-growing and larger tumors than homogeneous (Con, constitutive) angiogenesis. (*H*) Spatial patterns of predicted levels of VEGFA secretion for responsive and constitutive strategies. (*I*) Growth rates and cost of secreting VEGFA for the two strategies. (*J* and *K*) Simulation results from an agent-based model. (*J*) Growth curves of tumors using different proangiogenic strategies confirmed that the responsive strategy leads to enhanced tumor growth compared with the constitutive strategy. *J*, *Right* shows representative images of model outcomes. The responsive strategy not only allowed for faster tumor growth, but also required less total VEGFA. (*K*) Bars indicate SD from 10 simulations. (*L*) Localized tube morphogenesis emerges within the MEMIC from a triple coculture of macrophages, endothelial cells (SVECs), and tumor cells (TS1, unlabeled). *L*, *Inset* shows a representative magnified region.

distribution of signals can be more relevant for the progression of the disease than its total levels, which could explain conflicting outcomes in anti-VEGFA therapies (12, 39). Our model also shows that tumors, by engaging with infiltrated macrophages, can activate a mechanism of revascularization that allows the delivery of nutrients where they are most needed without wasting resources in well-perfused tumor regions.

Our data and mathematical models suggest that proangiogenic conditions are restricted to ischemic regions, which would lead to local and responsive angiogenic strategies. To test this, we took advantage of the MEMIC system to generate regions of hypoxia in a triple coculture of PyMT-derived tumor cells, macrophages, and SVEC endothelial cells. After 3 d of culture, SVEC cells formed well-structured tubes but only within ischemic regions of the MEMIC (Fig. 4*L*). These data indicate that macrophages indeed orchestrate tube-like morphogenesis in regions where revascularization is most needed. More broadly, this suggests that macrophages conditioned by metabolic gradients can relay spatial information to neighboring cells, triggering functional adaptations to their local environment.

Discussion

Tumor progression is commonly seen as a deregulated, chaotic process, yet our data suggest that gradients of metabolites act as tumor morphogens and provide a local source of organization by inducing phenotypic patterns in macrophages. This process requires three simple conditions that are common in all solid tumors: alterations in cell metabolism, aberrant vascularization, and the presence of responsive stroma. These features lead to gradients of metabolites that orchestrate a coordinated and spatially organized angiogenic response.

It is possible that metabolite gradients also organize other cell types within the tumor microenvironment, including other immune cells (40–45) and malignant cells themselves. For example, low glutamine levels found in blood-deprived necrotic tumor cores lead to histone hypermethylation and dedifferentiation

of cancer cells (46). Extracellular metabolite sensing is at the core of biological organization and is conserved from bacteria to mammals (47). Thus, we speculate that metabolites represented the primal cues for positional information, which was then coopted by signaling molecules during metazoan evolution. Understanding the processes required for multicellular self-organization in tumors may allow identification of targetable features that are independent of specific genetic mutations and thus less prone to therapeutic resistance.

Materials and Methods

Cells were cultured under standard conditions, using DMEM supplemented with 10% (vol/vol) FBS. Images were acquired using an inverted wide-field fluorescent microscope (Zeiss AxioObserver.Z1) and the images were processed in Matlab, using custom-made analysis routines that are available upon request. All animal studies were performed using protocols approved by the Animal Care Committee at Memorial Sloan Kettering Cancer Center. Details about the analytical solution to the theoretical model can be found in *SI Materials and Methods*.

ACKNOWLEDGMENTS. We thank the entire J.B.X., J.A.J., and C.B.T. laboratories for useful discussions and feedback during the development of this project and on the manuscript. We specially thank Guillermina Altomonte, Ben Steventon, Wilhelm Palm, and Lydia Finley for critical reading of the manuscript. This work was supported by National Institutes of Health Grants R00CA191021 (to C.C.-F.), U54 CA209975 (to J.B.X.), and P30 CA008748 (Memorial Sloan Kettering Cancer Center Support Grant) and by a grant from the Geoffrey Beene Cancer Research Center (to J.B.X. and J.A.J.).

1. Lengauer C, Kinzler KW, Vogelstein B (1998) Genetic instabilities in human cancers. *Nature* 396(6712):643–649.
2. Marusyk A, Polyak K (2010) Tumor heterogeneity: Causes and consequences. *Biochim Biophys Acta Rev Canc* 1805(1):105–117.
3. Stephens PJ, et al. (2011) Massive genomic rearrangement acquired in a single catastrophic event during cancer development. *Cell* 144(1):27–40.
4. Gerlinger M, et al. (2012) Intratumor heterogeneity and branched evolution revealed by multiregion sequencing. *N Engl J Med* 366(10):883–892.
5. Burrell RA, McGranahan N, Bartek J, Swanton C (2013) The causes and consequences of genetic heterogeneity in cancer evolution. *Nature* 501(7467):338–345.
6. Laughney Ashley M, Elizalde S, Genovese G, Bakhoum SF (2015) Dynamics of tumor heterogeneity derived from clonal karyotypic evolution. *Cell Rep* 12(5):809–820.
7. Gundem G, et al. (2015) The evolutionary history of lethal metastatic prostate cancer. *Nature* 520(7547):353–357.
8. Zhang C-Z, et al. (2015) Chromothripsis from DNA damage in micronuclei. *Nature* 522(7555):179–184.
9. Tabassum DP, Polyak K (2015) Tumorigenesis: It takes a village. *Nat Rev Cancer* 15(8):473–483.
10. Egeblad M, Nakasone ES, Werb Z (2010) Tumors as organs: Complex tissues that interface with the entire organism. *Dev Cell* 18(6):884–901.
11. Carmeliet P, Jain RK (2000) Angiogenesis in cancer and other diseases. *Nature* 407(6801):249–257.
12. Carmeliet P, Jain RK (2011) Principles and mechanisms of vessel normalization for cancer and other angiogenic diseases. *Nat Rev Drug Discov* 10(6):417–427.
13. Friedl P, Alexander S (2011) Cancer invasion and the microenvironment: Plasticity and reciprocity. *Cell* 147(5):992–1009.
14. Marusyk A, et al. (2014) Non-cell-autonomous driving of tumour growth supports sub-clonal heterogeneity. *Nature* 514(7520):54–58.
15. Cleary AS, Leonard TL, Gestl SA, Gunther EJ (2014) Tumour cell heterogeneity maintained by cooperating subclones in Wnt-driven mammary cancers. *Nature* 508(7494):113–117.
16. Vander Heiden MG, Cantley LC, Thompson CB (2009) Understanding the Warburg effect: The metabolic requirements of cell proliferation. *Science* 324(5930):1029–1033.
17. Koppenol WH, Bounds PL, Dang CV (2011) Otto Warburg's contributions to current concepts of cancer metabolism. *Nat Rev Cancer* 11(5):325–337.
18. Pavlova NN, Thompson CB (2016) The emerging hallmarks of cancer metabolism. *Cell Metab* 23(1):27–47.
19. Thomlinson RH, Gray LH (1955) The histological structure of some human lung cancers and the possible implications for radiotherapy. *Br J Cancer* 9(4):539–549.
20. Gatenby RA, Gillies RJ (2004) Why do cancers have high aerobic glycolysis? *Nat Rev Cancer* 4(11):891–899.
21. Carmona-Fontaine C, et al. (2013) Emergence of spatial structure in the tumor microenvironment due to the Warburg effect. *Proc Natl Acad Sci USA* 110(48):19402–19407.
22. Colegio OR, et al. (2014) Functional polarization of tumour-associated macrophages by tumour-derived lactic acid. *Nature* 513(7519):559–563.
23. Lewis C, Murdoch C (2005) Macrophage responses to hypoxia: Implications for tumor progression and anti-cancer therapies. *Am J Pathol* 167(3):627–635.
24. Wenes M, et al. (2016) Macrophage metabolism controls tumor blood vessel morphogenesis and metastasis. *Cell Metab* 24(5):701–715.
25. Joyce JA, Pollard JW (2009) Microenvironmental regulation of metastasis. *Nat Rev Cancer* 9(4):239–252.
26. Qian BZ, Pollard JW (2010) Macrophage diversity enhances tumor progression and metastasis. *Cell* 141(1):39–51.
27. Mantovani A, Allavena P, Sica A, Balkwill F (2008) Cancer-related inflammation. *Nature* 454(7203):436–444.
28. Gordon S (2003) Alternative activation of macrophages. *Nat Rev Immunol* 3(1):23–35.
29. Lawrence T, Natoli G (2011) Transcriptional regulation of macrophage polarization: Enabling diversity with identity. *Nat Rev Immunol* 11(11):750–761.
30. Wolpert L (1969) Positional information and the spatial pattern of cellular differentiation. *J Theor Biol* 25(1):1–47.
31. Green JB, Sharpe J (2015) Positional information and reaction-diffusion: Two big ideas in developmental biology combine. *Development* 142(7):1203–1211.
32. Briscoe J, Small S (2015) Morphogen rules: Design principles of gradient-mediated embryo patterning. *Development* 142(23):3996–4009.
33. Mayor R, Carmona-Fontaine C (2010) Keeping in touch with contact inhibition of locomotion. *Trends Cell Biol* 20(6):319–328.
34. El Kasmi KC, et al. (2008) Toll-like receptor-induced arginase 1 in macrophages thwarts effective immunity against intracellular pathogens. *Nat Immunol* 9(12):1399–1406.
35. Ashe HL, Briscoe J (2006) The interpretation of morphogen gradients. *Development* 133(3):385–394.
36. Rogers KW, Schier AF (2011) Morphogen gradients: From generation to interpretation. *Annu Rev Cell Dev Biol* 27(1):377–407.
37. Cattin AL, et al. (2015) Macrophage-induced blood vessels guide Schwann cell-mediated regeneration of peripheral nerves. *Cell* 162(5):1127–1139.
38. Secomb TW, Alberding JP, Hsu R, Dewhirst MW, Pries AR (2013) Angiogenesis: An adaptive dynamic biological patterning problem. *PLoS Comput Biol* 9(3):e1002983.
39. Lu-Emerson C, et al. (2015) Lessons from anti-vascular endothelial growth factor and anti-vascular endothelial growth factor receptor trials in patients with glioblastoma. *J Clin Oncol* 33(10):1197–1213.
40. O'Neill LAJ, Hardie DG (2013) Metabolism of inflammation limited by AMPK and pseudo-starvation. *Nature* 493(7432):346–355.
41. Pearce EL, Poffenberger MC, Chang CH, Jones RG (2013) Fueling immunity: Insights into metabolism and lymphocyte function. *Science* 342(6155):1242454.
42. O'Neill LAJ, Pearce EJ (2016) Immunometabolism governs dendritic cell and macrophage function. *J Exp Med* 213(1):15–23.
43. Siska PJ, Rathmell JC (2015) T cell metabolic fitness in antitumor immunity. *Trends Immunol* 36(4):257–264.
44. Chang C-H, Pearce EL (2016) Emerging concepts of T cell metabolism as a target of immunotherapy. *Nat Immunol* 17(4):364–368.
45. Brand A, et al. (2016) LDHA-associated lactic acid production blunts tumor immunosurveillance by T and NK cells. *Cell Metab* 24(5):657–671.
46. Pan M, et al. (2016) Regional glutamine deficiency in tumours promotes dedifferentiation through inhibition of histone demethylation. *Nat Cell Biol* 18(10):1090–1101.
47. Chantranupong L, Wolfson RL, Sabatini DM (2015) Nutrient-sensing mechanisms across evolution. *Cell* 161(1):67–83.
48. Lee Dong C, et al. (2015) A lactate-induced response to hypoxia. *Cell* 161(3):595–609.
49. Brader P, et al. (2007) Imaging of hypoxia-driven gene expression in an orthotopic liver tumor model. *Mol Cancer Ther* 6:2900–2908.
50. Gocheva V, et al. (2010) IL-4 induces cathepsin protease activity in tumor-associated macrophages to promote cancer growth and invasion. *Genes Dev* 24:241–255.
51. Lopez T, Hanahan D (2002) Elevated levels of IGF-1 receptor convey invasive and metastatic capability in a mouse model of pancreatic islet tumorigenesis. *Cancer Cell* 1:339–353.
52. Bong KW, et al. (2012) Non-polydimethylsiloxane devices for oxygen-free flow lithography. *Nat Commun* 3:805.
53. Cox ME, Dunn B (1986) Oxygen diffusion in poly(dimethyl siloxane) using fluorescence quenching. I. Measurement technique and analysis. *J Polym Sci A Polym Chem* 24:621–636.
54. Schmitt TM, Zuniga-Pflucker JC (2002) Induction of T cell development from hematopoietic progenitor cells by delta-like-1 in vitro. *Immunity* 17:749–756.
55. Love MI, Huber W, Anders S (2014) Moderated estimation of fold change and dispersion for RNA-seq data with DESeq2. *Genome Biol* 15:550.
56. Anderson AR, Weaver AM, Cummings PT, Quaranta V (2006) Tumor morphology and phenotypic evolution driven by selective pressure from the microenvironment. *Cell* 127:905–915.
57. Enderling H, Hlatky L, Hahnfeldt P (2010) Tumor morphological evolution: Directed migration and gain and loss of the self-metastatic phenotype. *Biol Direct* 5:23.
58. Basanta D, Anderson AR (2013) Exploiting ecological principles to better understand cancer progression and treatment. *Interface Focus* 3(4):20130020.
59. Xavier JB, Picioreanu C, Van Loosdrecht MCM (2005) A framework for multidimensional modelling of activity and structure of multispecies biofilms. *Environ Microbiol* 7:1085–1103.
60. Xavier JB, de Kreuk MK, Picioreanu C, van Loosdrecht MCM (2007) Multi-scale individual-based model of microbial and bioconversion dynamics in aerobic granular sludge. *Environ Sci Technol* 41:6410–6417.
61. Jain M, et al. (2012) Metabolite profiling identifies a key role for glycine in rapid cancer cell proliferation. *Science* 336:1040–1044.
62. Intlekofer A, et al. (2015) Hypoxia induces production of L-2-hydroxyglutarate. *Cell Metab* 22:304–311.
63. Chouchani ET, et al. (2014) Ischaemic accumulation of succinate controls reperfusion injury through mitochondrial ROS. *Nature* 515:431–435.